BIOCHEMISTRY
including biophysical chemistry & molecular biology

ACCELERATED PUBLICATION

pubs.acs.org/biochemistry

Crystallographic and Kinetic Evidence of Allostery in a Trypsin-like Protease

Weiling Niu, Zhiwei Chen, Prafull S. Gandhi, Austin D. Vogt, Nicola Pozzi, Leslie A. Pelc, Fatima Zapata, and Enrico Di Cera*

Department of Biochemistry and Molecular Biology, Saint Louis University School of Medicine, St. Louis, Missouri 63104, United States

ABSTRACT: Protein allostery is based on the existence of multiple conformations in equilibrium linked to distinct functional properties. Although evidence of allosteric transitions is relatively easy to identify by functional studies, structural detection of a pre-existing equilibrium between alternative conformations remains challenging even for textbook examples of allosteric proteins. Kinetic studies show that the trypsin-like protease thrombin exists in equilibrium between two conformations where the active site is either collapsed (E*) or accessible to substrate (E). However, structural demonstration that the two conformations exist in the same enzyme construct free of ligands has remained elusive. Here we report the crystal structure of the thrombin mutant N143P in the E form, which complements the recently reported structure in the E* form, and both the E and E* forms of the thrombin mutant Y225P. The side chain of W215 moves 10.9 Å between the two forms, causing a displacement of 6.6 Å of the entire 215−217 segment into the active site that in turn opens or closes access to the primary specificity pocket. Rapid kinetic measurements of *p*-aminobenzamidine binding to the active site confirm the existence of the E*−E equilibrium in solution for wild-type and the mutants N143P and Y225P. These findings provide unequivocal proof of the allosteric nature of thrombin and lend strong support to the recent proposal that the E*−E equilibrium is a key property of the trypsin fold.

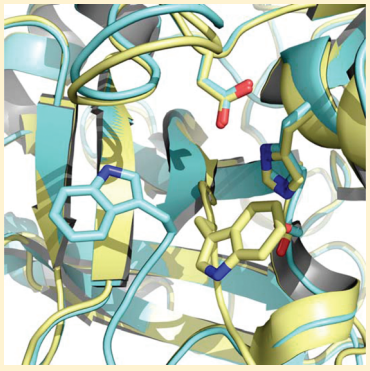

The hallmark of allosteric proteins is that they exist in multiple conformations in equilibrium.[1,2] When alternative conformations differ in their functional properties, linkage is established between structure and biological activity and allostery becomes the basis of the effects observed experimentally. The theoretical underpinnings of allosteric transitions have been defined for systems working at equilibrium [1] or under transient kinetics.[3] Yet structural validation of a pre-existing equilibrium between alternative conformations remains a challenge even for textbook examples of allosteric proteins.[2,4]

Allostery is not an exclusive property of multimeric proteins. Indeed, the ability of monomeric enzymes to express complex behavior consistent with allosteric transitions has long been recognized.[3,5] Trypsin-like proteases are monomeric enzymes which constitute the largest and best studied group of homologous proteases in the human genome.[6] They are phylogenetically grouped into six functional categories: digestion, coagulation and immunity, tryptase, matriptase, kallikrein, and granzymes. Trypsin-like proteases share a common mechanism of catalysis that relies upon the coordinate action of three catalytic residues: H57, D102, and S195 (chymotrypsinogen numbering). In addition, they share a common mechanism of activation: an inactive zymogen precursor is proteolytically cut between residues 15 and 16 to generate a new N-terminus that ion-pairs with the highly conserved D194 next to the catalytic S195 and organizes both the oxyanion hole and primary specificity pocket.[6−8]

The irreversible zymogen→protease conversion affords a useful paradigm to explain the onset of catalytic activity as seen in the digestive system, blood coagulation, or the complement system and is particularly useful to understand the initiation, progression, and amplification of enzyme cascades, where each component acts as a substrate in the inactive zymogen form in one step and as an active enzyme in the subsequent step.[9] However, considerable variation in catalytic activity is observed among members of the trypsin family following conversion from the inactive zymogen form. Digestive enzymes such as trypsin, chymotrypsin, and elastase complement factors C1r and C1s, and coagulation factors like thrombin are highly active after the zymogen→protease conversion has taken place. On the other hand, complement factors B and C2 are mostly inactive until binding of complement factors C3b and C4b enable catalytic activity at the site where amplification of C3 activation leads to formation of the membrane attack complex.[10−12] Coagulation factor VIIa circulates in the blood as a poorly active protease that acquires full catalytic competence only upon interaction with tissue factor that becomes exposed to the bloodstream upon vascular injury.[13,14] Complement factor D assumes an inactive conformation with a distorted catalytic triad [15,16] until binding to C3b and factor B promote substrate binding and catalytic

Received: June 7, 2011
Revised: June 25, 2011
Published: June 28, 2011

Table 1. Crystallographic Data for Thrombin Mutants N143P and Y225P

	N143P - E form	N143P - E* form	Y225P - E form	Y225P - E* form
Buffer/salt	0.2 M NH_4I	0.1 M imidazole	0.2 M K formate	0.1 M Tris, pH 8.0
PEG	3350 (20%)	8000 (7%)	3350 (20%)	8000 (8%)
PDB ID	3QGN	3JZ2	3S7K	3S7H
Data collection:	Raxis IV^{++}	Mar345	Raxis IV^{++}	Raxis IV^{++}
Wavelength (Å)	1.54	1.54	1.54	1.54
Space group	*C*2	$P4_3$	$P2_12_12$	$P4_3$
Unit cell dimensions (Å)	*a* = 122.2	*a* = 57.9	*a* = 61.9	*a* = 57.6
	b = 48.0	*b* = 57.9	*b* = 86.8	*b* = 57.6
	c = 52.0	*c* = 119.8	*c* = 101.0	*c* = 119.9
	β = 94.3°			
Molecules/asymmetric unit	1	1	2	1
Resolution range (Å)	40−2.1	40−2.4	40−1.9	40−1.9
Observations	75156	83891	286602	185752
Unique observations	17583	14942	43419	30093
Completeness (%)	98.5 (97.3)	96.7 (77.8)	99.3 (98.2)	97.8 (86.3)
R_{sym} (%)	10.5 (16.0)	7.6 (40.8)	5.4 (30.5)	7.3 (41.8)
$I/\sigma(I)$	13.3 (6.6)	19.0 (2.2)	27.6 (4.0)	20.7 (2.4)
Refinement:				
Resolution (Å)	40−2.1	40−2.4	40−1.9	40−1.9
R_{cryst}, R_{free}	0.189, 0.239	0.189, 0.246	0.175, 0.216	0.175, 0.204
Reflections (working/test)	15588/892	14167/747	38897/2179	27031/1518
Protein atoms	2253	2242	4589	2273
Solvent molecules	150	116	382	191
Rmsd bond lengths[a] (Å)	0.010	0.012	0.010	0.0080
Rmsd angles[a] (deg)	1.3	1.4	1.3	1.1
Rmsd ΔB (Å^2) (mm/ms/ss)[b]	2.99/2.28/3.26	2.02/1.36/2.45	2.18/1.83/2.70	2.86/2.33/2.56
$\langle B \rangle$ protein (Å^2)	41.8	34.1	35.4	39.0
$\langle B \rangle$ solvent (Å^2)	52.1	20.3	45.2	52.6
Ramachandran plot:				
Most favored (%)	99.2	100	99.6	100
Generously allowed (%)	0.4	0	0.2	0
Disallowed (%)	0.4	0	0.2	0

[a] Root-mean-squared deviation (Rmsd) from ideal bond lengths and angles and Rmsd in *B*-factors of bonded atoms. [b] mm, main chain−main chain; ms, main chain−side chain; ss, side chain−side chain. The structure of N143P in the E* form is from ref 29.

activity.[17,18] The high catalytic activity of trypsin, C1r, and thrombin and the ability of complement factor D or coagulation factor VIIa to remain in a zymogen-like form suggest that the trypsin fold may assume active and inactive conformations even after the zymogen→protease conversion has taken place. Existence of an allosteric equilibrium between active and inactive forms has been proposed for coagulation factor VIIa.[14,19] Rapid kinetics support a pre-existing equilibrium between active (E) and inactive (E*) forms for thrombin,[20,21] meizothrombin desF1,[22] factor Xa, and activated protein C.[23] Structures of thrombin in the free form reveal a conformation, E, with the active site open [24−26] and an alternative conformation, E*, with the active site blocked by repositioning of the 215−217 segment.[27−30] However, no evidence currently exists that the same protease construct may assume alternative conformations that can be trapped by crystallographic analysis. This evidence is reported here for the first time.

MATERIALS AND METHODS

Thrombin mutants N143P and Y225P were expressed in mammalian cells or *E. coli* and purified to homogeneity as described previously.[29,31] Crystallization was achieved at 22 °C using the hanging drop vapor diffusion method, with each reservoir containing 500 μL of solution. Equal volumes (2 μL) of the protein sample (8−9 mg/mL) and reservoir solution (see Table 1) were mixed to prepare the hanging drops. Diffraction quality crystals grew in two weeks and were frozen using 15%−25% glycerol as cryoprotectant at 100 K. X-ray diffraction data were collected to 1.9−2.1 Å with a home source (Rigaku 1.2 kW MMX007 generator with VHF optics) Rigaku Raxis IV^{++} detector and were indexed, integrated, and scaled with the HKL2000 software package.[32] Structures were solved by molecular replacement using MOLREP from the CCP4 suite [33] and using as search models PDB accession code 3JZ1 for N143P in the E form, 1SHH for Y225P in the E form,

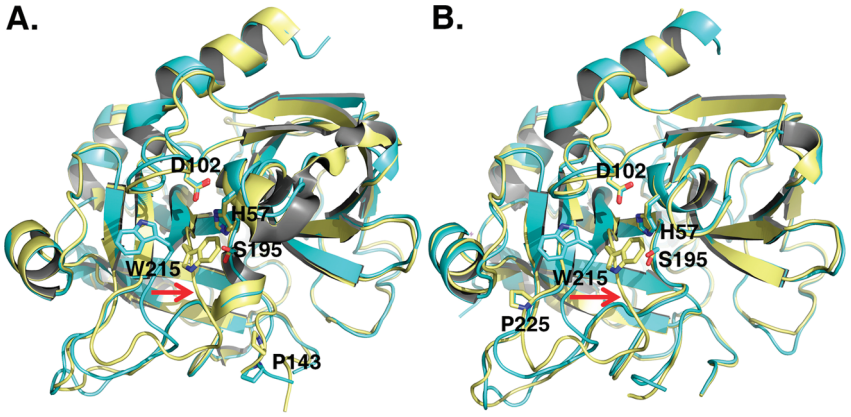

Figure 1. X-ray crystal structures of the thrombin mutants N143P and Y225P in the E* and E forms. Ribbon representation of the structure of the thrombin mutants N143P (A) and Y225P (B) in the E (cyan) and E* (gold) forms. In the E* form the side chain of W215 and the entire 215−217 segment collapse into the active site (red arrow). In the E form, W215 moves back 10.9 Å and the 215−217 segment moves 6.6 Å to make the active site accessible to substrate. The rmsd between the two forms is 0.328 Å (N143P) or 0.345 Å (Y225P). Relevant residues are labeled and rendered as sticks.

and 3BEI for Y225P in the E* form. Refinement and electron density generation were performed with REFMAC [34] from the CCP4 suite, and 5% of the reflections were randomly selected as a test set for cross-validation. Model building was performed in COOT.[35] In the final stage of refinement, TLS tensors modeling rigid-body anisotropic temperature factors were calculated and applied to the model. Ramachandran plots were calculated using PROCHECK.[36] Statistics for data collection and refinement are summarized in Table 1. Atomic coordinates and structure factors have been deposited in the PDB as 3QGN (N143P E form), 3S7K (Y225P E form), and 3S7H (Y225P E* form).

Stopped-flow fluorescence measurements of PABA binding to thrombin were performed over a time range of 100 ms using an Applied Photophysics SX20 spectrometer. An excitation wavelength of 330 nm and a cutoff filter of 375 nm were used for the experiments. All experiments were carried out in buffer containing 50 mM Tris, 0.1% PEG8000, pH 8.0 at 15 °C. Thrombin wild type or mutant at a final concentration of 1 μM was mixed 1:1 with increasing concentrations of PABA, having first established a baseline by mixing buffer and the same concentration of PABA. Applied Photophysics Pro-Data software was used to fit single exponential curves to the average of six or more kinetic traces for each PABA concentration. PABA was found to obey a two-step binding mechanism, with a fast phase too rapid to resolve and a slow, single exponential phase whose k_{obs} decreases with increasing [PABA]. This dependence of the slow phase on ligand concentration is unequivocal proof of the kinetic mechanism of binding[20]

$$E^* \underset{k_r}{\overset{k_{-r}}{\rightleftharpoons}} E \underset{k_1[L]}{\overset{k_{-1}}{\rightleftharpoons}} EL$$

which is analogous to the binding mechanism of Na^+. A preequilibrium between two forms, E* and E, precedes PABA (L) binding that can only occur to the active form E. The total fluorescence change observed upon PABA binding obeys the expression[20]

$$F = \frac{F_0 + F_1 K_{app}[PABA]}{1 + K_{app}[PABA]} \quad (1)$$

where F_0 and F_1 are the values of F at [PABA] = 0 and [PABA] = ∞, and

$$K_{app} = \frac{[E : PABA]}{([E^*] + [E])[PABA]} = \frac{K_A}{1 + r} \quad (2)$$

is the apparent PABA binding affinity that depends on the intrinsic PABA binding affinity K_A = [E:PABA]/[E][PABA] and the equilibrium constant for the E*−E interconversion r = [E*]/[E] = $(k_{-r})/(k_r)$. Under conditions of separation of time scales, where PABA binding and dissociation are faster than the rates for the E*−E interconversion, the k_{obs} for the evolution of the slow phase of fluorescence increase upon PABA binding obeys the expression

$$k_{obs} = k_r + k_{-r}\frac{1}{1 + K_A[PABA]} \quad (3)$$

The value of k_{obs} decreases hyperbolically with increasing [PABA] from $k_r + k_{-r}$ ([PABA] = 0) to k_r ([PABA] = ∞), thereby yielding k_r, k_{-r}, and K_A.

RESULTS AND DISCUSSION

Structures of thrombin in the free form reveal a conformation with the active site fully accessible to substrate [24−26] and an alternative conformation with the active site blocked by repositioning of the W215 side chain and entire 215−217 segment.[27−30] Although these conformations provide a structural basis for the allosteric E*−E equilibrium identified by kinetic studies,[20,21,23] they have been documented with different protease constructs. The mutant N143P was engineered to abrogate the H-bond between the carbonyl O atom of E192 and the backbone N-atom of N143, resulting in a flip of the E192-G193 peptide bond and disruption of the oxyanion hole formed by the backbone N-atoms of G193 and S195.[29] A recently published structure of N143P in the free form reveals the predicted disruption of the oxyanion hole and a collapsed architecture of the active site (Figure 1) as observed in the E* form of the thrombin mutants D102N [28,30] and Δ146−149e.[27] The new structure of N143P in the free form reveals an open conformation of the active site (Figure 1), consistent with that observed in the E form of mutants R77aA [25] and

C191A/C220A.[24] The side chain of W215 moves back >10 Å toward F227 and relinquishes its interaction with the catalytic H57. The entire 215−217 segment moves >6 Å and opens up access to the active site. The mutant Y225P was engineered to abolish Na^+ binding and constitutively stabilize thrombin in the Na^+-free slow form.[37,38] Residue 225 has a dichotomous distribution in trypsin-like proteases: Pro is the preferred residue at this position, but Na^+ binding requires the presence of Tyr or Phe as seen in clotting and complement proteases. The slow form is the form of thrombin free of any ligands, and based on the results of rapid kinetics, it is a mixture of the inactive E* and active E forms. The mutant was crystallized previously bound to an active site inhibitor.[39] The new structures of Y225P in the free form reveal the two conformations, E and E*, analogous to those documented for N143P (Figure 1), thereby confirming that free thrombin (or slow thrombin) is a mixture of E* and E in allosteric equilibrium as predicted by kinetic studies on the wild-type,[20]

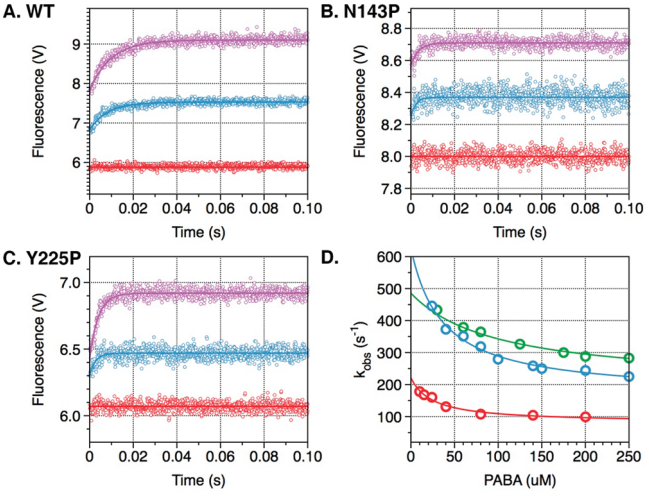

Figure 2. PABA binding to thrombin wild type and mutants N143P and Y225P. Kinetic traces of PABA binding to thrombin wild type (A) and mutants N143P (B) and Y225P (C). In all cases, binding of PABA obeys a two-step mechanism, with a fast phase completed within the dead time (<0.5 ms) of the spectrometer, followed by a single-exponential slow phase. Traces were recorded in the presence of 40 μM (cyan) or 200 μM (purple) PABA. Controls with 200 μM PABA in buffer are shown in red. (D) The k_{obs} for the slow phase decreases with increasing [PABA]. The values were obtained from analysis of the kinetic traces (A-C) and analyzed according to eq 3 in the text with best-fit parameter values reported in Table 2 for wild type (red), N143P (green) and Y225P (cyan). Experimental conditions are: 1 μM enzyme, 50 mM Tris, 0.1% PEG8000, pH 8.0, at 15 °C. The value of k_{obs} features an inverse hyperbolic dependence on [PABA], thereby proving the existence of the E*−E equilibrium preceding PABA binding.

The E*−E equilibrium was originally discovered from rapid kinetic studies of Na^+ binding to thrombin,[20] recently extended to meizothrombin desF1,[22] activated protein C, and factor Xa.[23] Because Na^+ cannot bind to the mutant Y225P due to the shift in the carbonyl O-atom of K224 caused by the presence of P225,[37] an alternative probe of the E*−E equilibrium becomes necessary. Such a probe could have wide applicability to trypsin-like proteases in general because Pro is the residue most represented at the 225 position in these enzymes [40] and Na^+ activation is present only in a minority of enzymes in blood coagulation and the complement cascade.[41] The active site inhibitor PABA has long been known as a useful reagent in fluorescence studies [42] and turned out to be an excellent probe of the accessibility of the active site in the E and E* forms (Figure 2). Rapid kinetics of PABA binding to wild-type thrombin reveals a two-step mechanism analogous to that observed for Na^+ binding, with a fast phase completed within the dead time of the instrument and a slow phase of exponential increase in fluorescence whose k_{obs} decreases hyperbolically as a function of [PABA] (Figure 2). This is an unequivocal signature of the existence of a pre-equilibrium that precedes PABA binding to the enzyme, and it likely reports the same E*−E equilibrium detected from Na^+ binding measurements. Indeed, the rate constants for the E*−E interconversion derived from measurements of PABA binding (Table 2) are comparable to those derived from Na^+ binding. Hence, the E*−E equilibrium in solution can be probed independently by binding to two different domains of the enzyme, the Na^+ site or the active site. Rapid kinetic measurements of PABA binding to the mutants N143P and Y225P also reveal a slow phase with a k_{obs} decreasing hyperbolically with increasing [PABA], thereby enabling detection of the E*−E equilibrium in systems where either Na^+ cannot bind to its site (Y225P) or Na^+ binding does not elicit a slow kinetic phase (N143P).[29] This offers a powerful new strategy to probe the E*−E equilibrium in other trypsin-like proteases.

The relevance of these findings carries over to the entire family of trypsin-like proteases to which thrombin belongs. Indeed, a recent analysis of the entire structural database demonstrates that the E*−E equilibrium is a general feature of the trypsin fold, made possible by the conformational flexibility of W215 and the 215−217 segment.[43] The E* form has been observed in the thrombin mutants D102N,[28,30] Δ146−149e,[27] N143P,[29] and Y225P reported here, complement factor D wild-type and mutants S915A, S215W, and R218A,[16−18] prostate specific antigen,[44] tonin,[45] prophenoloxidase activating factor II,[46] hepatocyte growth factor activator, [47] and prostasin.[48,49] The E form has been observed in the thrombin mutants R77aA,[25,26] C191A/C220A,[24] and N143P and Y225P reported here, complement factors C1r [50] and C2a,[51,52] neuropsin,[53] and trypsin.[54] Mutant D216G of αI-tryptase crystallizes with the 215−217 segment in two conformations in a 3:1 occupancy ratio:[55] one open and the

Table 2. Parameters for PABA to Thrombin Wild Type and Mutants N143P and Y225P

Enzyme	F_0 (V)[a]	F_1 (V)[a]	$\Delta F/F_0$ (%)[a]	K_{app} (mM^{-1})[a]	K_A (mM^{-1})[b]	k_r (s^{-1})[b]	k_{-r} (s^{-1})[b]	r[b]
wt	6.66 ± 0.04	9.70 ± 0.03	46	17 ± 1	40 ± 2	91 ± 2	120 ± 10	1.3 ± 0.1
N143P	8.25 ± 0.05	9.20 ± 0.05	12	4.0 ± 0.3	10 ± 1	200 ± 10	290 ± 10	1.5 ± 0.2
Y225P	5.96 ± 0.03	7.20 ± 0.04	21	7.6 ± 0.5	28 ± 2	170 ± 10	460 ± 20	2.7 ± 0.3

[a] From the data in Figure 3A−C using eq 1 in the text. [b] From the data in Figure 2D using eq 3 in the text. The values of k_r and k_{-r} derived for wild-type from rapid kinetics of Na^+ binding are 89 ± 2 s^{-1} and 85 ± 9 s^{-1}.[23]

dx.doi.org/10.1021/bi200878c |*Biochemistry* 2011, 50, 6301–6307

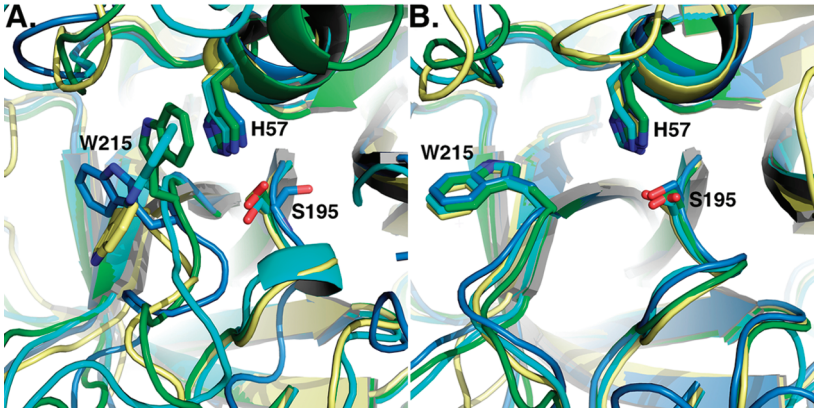

Figure 3. E* and E in the trypsin fold. Active site conformations of relevant trypsin-like proteases in the E* form (A) or the E form (B). Note how the active site is fully open in the E form (B) but occluded to various degrees in the E* form (A). Structures are colored as follows: (A) prostasin (3DFJ, yellow), thrombin mutant N143P (3JZ2, cyan), complement factor D mutant S215W (1DST, green), prophenoloxidase activating factor II (2B9L, blue), (B) complement factor C1r (1MD8, yellow), thrombin mutant N143P (cyan, 3QGN), neuropsin (1NPM, green), trypsin (2G51, blue).

other collapsed as in the wild-type.[56] Relevant examples of these proteases in the E and E* forms are given in Figure 3. Detection of E* and E for the same protease construct remains challenging because it requires crystallization of the free form under conditions where either E* or E can be trapped. However, this difficulty can be overcome, as shown by the thrombin mutants N143P and Y225P reported here, and we expect more trypsin-like proteases to be crystallized in both the E* and E forms in the near future.

The physiological relevance of the E*−E equilibrium deserves attention. When E* is stabilized, the protease possesses low activity and acts as a switch that can be turned on by binding of specific cofactors or allosteric activators that facilitate conversion to the active E form. Relevant examples are complement factor D that shifts from the E* to the E form upon binding to the complex of C3b and factor B [17] and coagulation factor VIIa that makes a similar transition upon binding to tissue factor.[14,19] Stabilization of E produces a highly active enzyme upon conversion from the zymogen form without requiring macromolecular cofactors, as seen in trypsin, complement factor C1r, and thrombin. Therefore, the E*−E equilibrium provides a reversible mechanism of regulation of enzyme activity following the irreversible transition from the zymogen form. The repertoire of activities available to the protease is greatly expanded in ways that fit the diverse requirements of enzymes acting in different biological environments or at different levels of cascades like blood coagulation and the complement.

AUTHOR INFORMATION

Corresponding Author

*E-mail: enrico@slu.edu. Telephone: 314 977 9201. Fax: 314 977 1183.

Funding Sources

This work was supported in part by the National Institutes of Health Research Grants HL49413, HL58141, HL73813, and HL95315 (to E.D.C.) and a PostDoctoral Research Fellowship from the American Heart Association (to W.N.).

ACKNOWLEDGMENT

We are grateful to Ms. Tracey Baird for her help with illustrations.

ABBREVIATIONS

PABA, *p*-aminobenzamidine; PDB, Protein Data Bank; PEG, polyethyleneglycol.

REFERENCES

(1) Monod, J., Wyman, J., and Changeux, J. P. (1965) On the nature of allosteric transitions: a plausible model. *J. Mol. Biol. 12*, 88–118.

(2) Perutz, M. F. (1989) Mechanisms of cooperativity and allosteric regulation in proteins. *Q. Rev. Biophys. 22*, 139–237.

(3) Frieden, C. (1970) Kinetic aspects of regulation of metabolic processes. The hysteretic enzyme concept. *J. Biol. Chem. 245*, 5788–5799.

(4) Fetler, L., Kantrowitz, E. R., and Vachette, P. (2007) Direct observation in solution of a preexisting structural equilibrium for a mutant of the allosteric aspartate transcarbamoylase. *Proc. Natl. Acad. Sci. U.S.A. 104*, 495–500.

(5) Botts, J., and Morales, M. (1953) Analytical description of the effects of modifiers and of multivalency upon the steady state catalyzed reaction rate. *Trans Faraday Soc 49*, 696–707.

(6) Page, M. J., and Di Cera, E. (2008) Serine peptidases: classification, structure and function. *Cell. Mol. Life Sci. 65*, 1220–1236.

(7) Hedstrom, L. (2002) Serine protease mechanism and specificity. *Chem Rev 102*, 4501–4524.

(8) Perona, J. J., and Craik, C. S. (1995) Structural basis of substrate specificity in the serine proteases. *Protein Sci. 4*, 337–360.

(9) Krem, M. M., and Di Cera, E. (2002) Evolution of enzyme cascades from embryonic development to blood coagulation. *Trends Biochem. Sci. 27*, 67–74.

(10) Gros, P., Milder, F. J., and Janssen, B. J. (2008) Complement driven by conformational changes. *Nat. Rev. Immunol. 8*, 48–58.

(11) Arlaud, G. J., Barlow, P. N., Gaboriaud, C., Gros, P., and Narayana, S. V. (2007) Deciphering complement mechanisms: the contributions of structural biology. *Mol. Immunol. 44*, 3809–3822.

(12) Ponnuraj, K., Xu, Y., Macon, K., Moore, D., Volanakis, J. E., and Narayana, S. V. (2004) Structural analysis of engineered Bb fragment of complement factor B: insights into the activation mechanism of the alternative pathway C3-convertase. *Mol. Cell 14*, 17–28.

(13) Banner, D. W., D'Arcy, A., Chene, C., Winkler, F. K., Guha, A., Konigsberg, W. H., Nemerson, Y., and Kirchhofer, D. (1996) The crystal structure of the complex of blood coagulation factor VIIa with soluble tissue factor. *Nature 380*, 41–46.

(14) Eigenbrot, C., Kirchhofer, D., Dennis, M. S., Santell, L., Lazarus, R. A., Stamos, J., and Ultsch, M. H. (2001) The factor VII zymogen structure reveals reregistration of beta strands during activation. *Structure 9*, 627–636.

(15) Jing, H., Macon, K. J., Moore, D., DeLucas, L. J., Volanakis, J. E., and Narayana, S. V. (1999) Structural basis of profactor D activation: from a highly flexible zymogen to a novel self-inhibited serine protease, complement factor D. *EMBO J. 18*, 804–814.

(16) Narayana, S. V., Carson, M., el-Kabbani, O., Kilpatrick, J. M., Moore, D., Chen, X., Bugg, C. E., Volanakis, J. E., and DeLucas, L. J. (1994) Structure of human factor D. A complement system protein at 2.0 A resolution. *J. Mol. Biol. 235*, 695–708.

(17) Forneris, F., Ricklin, D., Wu, J., Tzekou, A., Wallace, R. S., Lambris, J. D., and Gros, P. (2010) Structures of C3b in complex with factors B and D give insight into complement convertase formation. *Science 330*, 1816–1820.

(18) Jing, H., Babu, Y. S., Moore, D., Kilpatrick, J. M., Liu, X. Y., Volanakis, J. E., and Narayana, S. V. (1998) Structures of native and complexed complement factor D: implications of the atypical His57 conformation and self-inhibitory loop in the regulation of specific serine protease activity. *J. Mol. Biol. 282*, 1061–1081.

(19) Dickinson, C. D., Kelly, C. R., and Ruf, W. (1996) Identification of surface residues mediating tissue factor binding and catalytic function of the serine protease factor VIIa. *Proc. Natl. Acad. Sci. U.S.A. 93*, 14379–14384.

(20) Bah, A., Garvey, L. C., Ge, J., and Di Cera, E. (2006) Rapid kinetics of Na+ binding to thrombin. *J. Biol. Chem. 281*, 40049–40056.

(21) Di Cera, E. (2008) Thrombin. *Mol. Aspects Med. 29*, 203–254.

(22) Papaconstantinou, M. E., Gandhi, P. S., Chen, Z., Bah, A., and Di Cera, E. (2008) Na(+) binding to meizothrombin desF1. *Cell. Mol. Life Sci. 65*, 3688–3697.

(23) Vogt, A. D., Bah, A., and Di Cera, E. (2010) Evidence of the E*−E equilibrium from rapid kinetics of Na(+) binding to activated protein C and factor Xa. *J. Phys. Chem. B 114*, 16125–16130.

(24) Bush-Pelc, L. A., Marino, F., Chen, Z., Pineda, A. O., Mathews, F. S., and Di Cera, E. (2007) Important role of the Cys-191: Cys-220 disulfide bond in thrombin function and allostery. *J. Biol. Chem. 282*, 27165–27170.

(25) Pineda, A. O., Carrell, C. J., Bush, L. A., Prasad, S., Caccia, S., Chen, Z. W., Mathews, F. S., and Di Cera, E. (2004) Molecular dissection of Na+ binding to thrombin. *J. Biol. Chem. 279*, 31842–31853.

(26) Pineda, A. O., Savvides, S. N., Waksman, G., and Di Cera, E. (2002) Crystal structure of the anticoagulant slow form of thrombin. *J. Biol. Chem. 277*, 40177–40180.

(27) Bah, A., Carrell, C. J., Chen, Z., Gandhi, P. S., and Di Cera, E. (2009) Stabilization of the E* form turns thrombin into an anticoagulant. *J. Biol. Chem. 284*, 20034–20040.

(28) Gandhi, P. S., Chen, Z., Mathews, F. S., and Di Cera, E. (2008) Structural identification of the pathway of long-range communication in an allosteric enzyme. *Proc. Natl. Acad. Sci. U.S.A. 105*, 1832–1837.

(29) Niu, W., Chen, Z., Bush-Pelc, L. A., Bah, A., Gandhi, P. S., and Di Cera, E. (2009) Mutant N143P reveals how Na+ activates thrombin. *J. Biol. Chem. 284*, 36175–36185.

(30) Pineda, A. O., Chen, Z. W., Bah, A., Garvey, L. C., Mathews, F. S., and Di Cera, E. (2006) Crystal structure of thrombin in a self-inhibited conformation. *J. Biol. Chem. 281*, 32922–32928.

(31) Marino, F., Pelc, L. A., Vogt, A., Gandhi, P. S., and Di Cera, E. (2010) Engineering thrombin for selective specificity toward protein C and PAR1. *J. Biol. Chem. 285*, 19145–19152.

(32) Otwinowski, Z., and Minor, W. (1997) Processing of X-ray diffraction data collected in oscillation mode. *Methods Enzymol. 276*, 307–326.

(33) Bailey, S. (1994) The CCP4 suite. Programs for protein crystallography. *Acta Crystallogr., Sect. D: Biol. Crystallogr. 50*, 760–763.

(34) Murshudov, G. N., Vagin, A. A., and Dodson, E. J. (1997) Refinement of macromolecular structures by the maximum-likelihood method. *Acta Crystallogr., Sect. D: Biol. Crystallogr. 53*, 240–255.

(35) Emsley, P., and Cowtan, K. (2004) Coot: model-building tools for molecular graphics. *Acta Crystallogr D Biol Crystallogr 60*, 2126–2132.

(36) Morris, A. L., MacArthur, M. W., Hutchinson, E. G., and Thornton, J. M. (1992) Stereochemical quality of protein structure coordinates. *Proteins 12*, 345–364.

(37) Dang, Q. D., and Di Cera, E. (1996) Residue 225 determines the Na(+)-induced allosteric regulation of catalytic activity in serine proteases. *Proc. Natl. Acad. Sci. U.S.A. 93*, 10653–10656.

(38) Dang, Q. D., Guinto, E. R., and Di Cera, E. (1997) Rational engineering of activity and specificity in a serine protease. *Nat. Biotechnol. 15*, 146–149.

(39) Guinto, E. R., Caccia, S., Rose, T., Futterer, K., Waksman, G., and Di Cera, E. (1999) Unexpected crucial role of residue 225 in serine proteases. *Proc. Natl. Acad. Sci. U.S.A. 96*, 1852–1857.

(40) Krem, M. M., and Di Cera, E. (2001) Molecular markers of serine protease evolution. *EMBO J. 20*, 3036–3045.

(41) Di Cera, E. (2006) A structural perspective on enzymes activated by monovalent cations. *J. Biol. Chem. 281*, 1305–1308.

(42) Evans, S. A., Olson, S. T., and Shore, J. D. (1982) *p*-Aminobenzamidine as a fluorescent probe for the active site of serine proteases. *J. Biol. Chem. 257*, 3014–3017.

(43) Gohara, D. W., and Di Cera, E. (2011) Allostery in trypsin-like proteases suggests new therapeutic strategies. *Trends Biotechnol*, in press.

(44) Carvalho, A. L., Sanz, L., Barettino, D., Romero, A., Calvete, J. J., and Romao, M. J. (2002) Crystal structure of a prostate kallikrein isolated from stallion seminal plasma: a homologue of human PSA. *J. Mol. Biol. 322*, 325–337.

(45) Fujinaga, M., and James, M. N. (1987) Rat submaxillary gland serine protease, tonin. Structure solution and refinement at 1.8 Å resolution. *J. Mol. Biol. 195*, 373–396.

(46) Piao, S., Song, Y. L., Kim, J. H., Park, S. Y., Park, J. W., Lee, B. L., Oh, B. H., and Ha, N. C. (2005) Crystal structure of a clip-domain serine protease and functional roles of the clip domains. *EMBO J. 24*, 4404–4414.

(47) Shia, S., Stamos, J., Kirchhofer, D., Fan, B., Wu, J., Corpuz, R. T., Santell, L., Lazarus, R. A., and Eigenbrot, C. (2005) Conformational lability in serine protease active sites: structures of hepatocyte growth factor activator (HGFA) alone and with the inhibitory domain from HGFA inhibitor-1B. *J. Mol. Biol. 346*, 1335–1349.

(48) Rickert, K. W., Kelley, P., Byrne, N. J., Diehl, R. E., Hall, D. L., Montalvo, A. M., Reid, J. C., Shipman, J. M., Thomas, B. W., Munshi, S. K., Darke, P. L., and Su, H. P. (2008) Structure of human prostasin, a target for the regulation of hypertension. *J. Biol. Chem. 283*, 34864–34872.

(49) Spraggon, G., Hornsby, M., Shipway, A., Tully, D. C., Bursulaya, B., Danahay, H., Harris, J. L., and Lesley, S. A. (2009) Active site conformational changes of prostasin provide a new mechanism of protease regulation by divalent cations. *Protein Sci. 18*, 1081–1094.

(50) Budayova-Spano, M., Grabarse, W., Thielens, N. M., Hillen, H., Lacroix, M., Schmidt, M., Fontecilla-Camps, J. C., Arlaud, G. J., and Gaboriaud, C. (2002) Monomeric structures of the zymogen and active catalytic domain of complement protease c1r: further insights into the c1 activation mechanism. *Structure 10*, 1509–1519.

(51) Krishnan, V., Xu, Y., Macon, K., Volanakis, J. E., and Narayana, S. V. L. (2007) The crystal structure of C2a, the catalytic fragment of classical pathway C3 and C5 convertase of human complement. *J. Mol. Biol. 367*, 224–233.

(52) Milder, F. J., Raaijmakers, H. C. A., Vandeputte, M. D. A. A., Schouten, A., Huizinga, E. G., Romijn, R. A., Hemrika, W., Roos, A., Daha, M. R., and Gros, P. (2006) Structure of complement component C2A: implications for convertase formation and substrate binding. *Structure 14*, 1587–1597.

(53) Kishi, T., Kato, M., Shimizu, T., Kato, K., Matsumoto, K., Yoshida, S., Shiosaka, S., and Hakoshima, T. (1999) Crystal structure of neuropsin, a hippocampal protease involved in kindling epileptogenesis. *J. Biol. Chem. 274*, 4220–4224.

(54) Mueller-Dieckmann, C., Panjikar, S., Schmidt, A., Mueller, S., Kuper, J., Geerlof, A., Wilmanns, M., Singh, R. K., Tucker, P. A., and Weiss, M. S. (2007) On the routine use of soft X-rays in macromolecular crystallography. Part IV. Efficient determination of anomalous substructures in biomacromolecules using longer X-ray wavelengths. *Acta Crystallogr., Sect. D: Biol. Crystallogr. 63*, 366–380.

(55) Rohr, K. B., Selwood, T., Marquardt, U., Huber, R., Schechter, N. M., Bode, W., and Than, M. E. (2006) X-ray structures of free and leupeptin-complexed human αI-tryptase mutants: indication for an α→*β*-tryptase transition. *J. Mol. Biol. 357*, 195–209.

(56) Marquardt, U., Zettl, F., Huber, R., Bode, W., and Sommerhoff, C. (2002) The crystal structure of human α1-tryptase reveals a blocked substrate-binding region. *J. Mol. Biol. 321*, 491–502.